ACS OMEGA

Open Access

This article is licensed under CC-BY-NC-ND 4.0

http://pubs.acs.org/journal/acsodf

Article

Water-Resistant Poly(vinyl alcohol)/ZnO Nanopillar Composite Films for Antibacterial Packaging

Yuanjian Xie, Pingxiong Cai,* Xiaofeng Cao, Bo Chen, and Yuanfeng Pan*

Cite This: *ACS Omega* 2024, 9, 50403−50413

Read Online

ACCESS | Metrics & More | Article Recommendations | Supporting Information

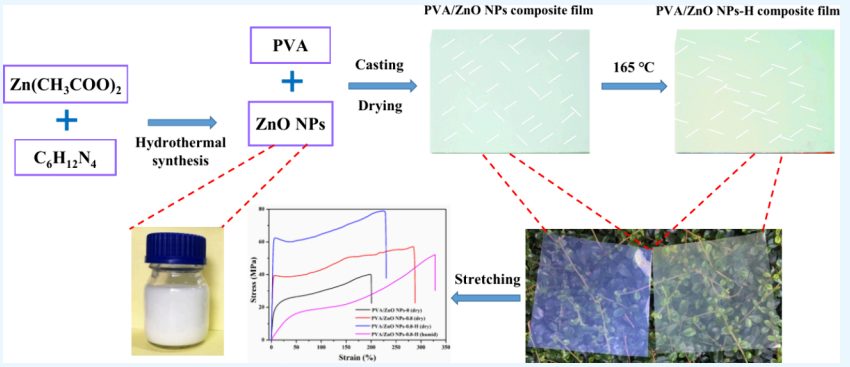

ABSTRACT: To solve the problems that poly(vinyl alcohol) (PVA) easily breeds bacteria and swells in a humid environment, PVA and ZnO nanopillar (ZnO NP) components were composed to generate PVA/ZnO NP composite films via a simple combination process of blending and heat treatment in this study. Here, ZnO NPs endowed composite films with good antibacterial properties, and the etherification and dehydration of hydroxyl groups between PVA molecular chains induced by heat treatment resulted in the composite films having excellent water-swelling resistance. Most importantly, PVA/ZnO NP composite films revealed excellent tensile strength in both humid (52.85 MPa) and dry (74.63 MPa) environments. In addition, PVA/ZnO NP composite films showed good antibacterial and antisepsis abilities as well as preservation functions in the packaging test of half-cut apples. The current work disclosed an easy strategy for producing a PVA-based antibacterial film for packaging materials that are water-resistant and highly strong, making them suitable for applications in humid environments.

1. INTRODUCTION

The versatile use of a petroleum-derived plastic film spans multiple industries, notably the packaging sector, delivering immense convenience to people's lives owing to its excellent physical and chemical attributes alongside its cost-effective production. The packaging industry is still dominated by conventional petroleum-derived plastic films, such as polystyrene and polyethylene.[1,2] On the other hand, these films are not biodegradable and are produced and used excessively by people; a significant amount of plastic trash is causing significant damage to the ecological environment of the Earth, like the marine environment.[3,4] In addition, the fact that a conventional petroleum-derived plastic film is produced using non-renewable petroleum resources raises an issue with its raw material restraints that cannot be disregarded. The packaging sector will be significantly impacted if a conventional petroleum-derived plastic film is no longer available due to either depletion of oil resources or disruptions in the supply chain or exploitation. Besides, bacterial contamination has been a concern during food packaging and storage.[5,6] Food packaging film materials having antibacterial properties not only package and preserve food but also significantly lower the chance of contamination of food by bacteria, particularly on the exterior of the packaging material. Thus, to mitigate and resolve the environmental issues brought on by conventional petroleum-derived plastic films and the presence of bacteria that contaminate food and to promote the sustainable growth of the packaging industry, the development of novel antibacterial packaging film materials that are cost-effective, practical, sustainable, and environmentally benign is imperative to supplant the conventional petroleum-based packaging films.[7,8]

Poly(vinyl alcohol) (PVA), which can be obtained by petroleum or non-petroleum routes, is a vinyl biodegradable polymer. PVA is a widely employed raw material for the production of ecologically acceptable packaging materials

Received: August 5, 2024
Revised: November 24, 2024
Accepted: December 2, 2024
Published: December 11, 2024

ACS Publications

© 2024 The Authors. Published by American Chemical Society

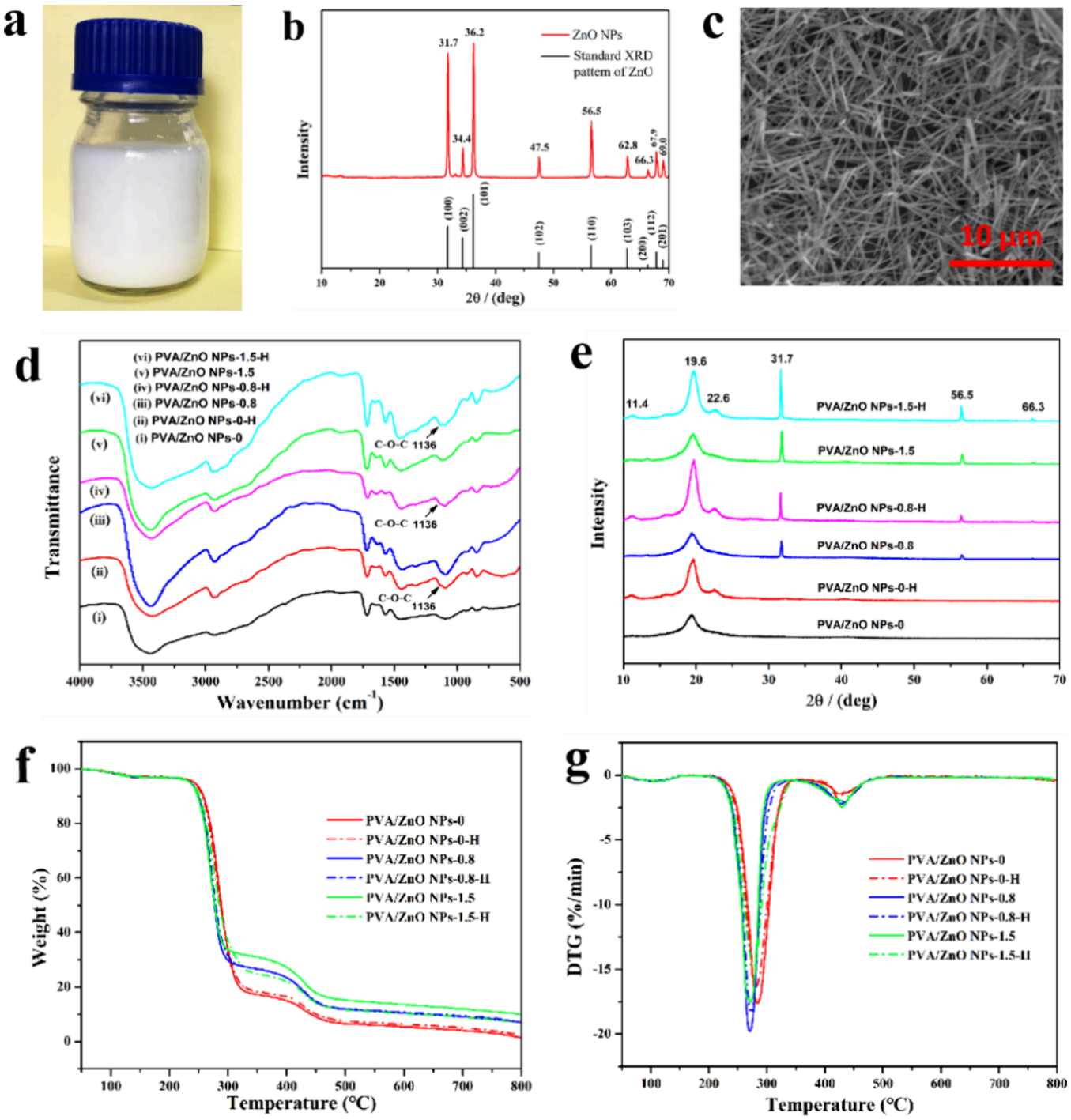

Figure 1. (a) 1 wt % aqueous dispersion, (b) XRD pattern, and (c) SEM image of the ZnO NPs and (d) FTIR spectra, (e) XRD patterns, (f) TGA curves, and (g) DTG curves of the PVA/ZnO NP composite films.

owing to its certain properties, such as flexibility, water solubility, biocompatibility, film-forming ability, resistance to chemical corrosion, and non-toxicity.[9−13] In comparison to traditional petroleum-based packaging materials, PVA films have certain limitations in packaging applications, such as poor water resistance. Poor water resistance will not only reduce the mechanical properties of PVA films but also easily breed bacteria, which significantly affects its packaging potential.[14,15] Therefore, boosting PVA films' ability to resist water and giving them antibacterial qualities is crucial for expanding their use in moist, humid conditions. For the enhancement of water resistance, heat treatment is a simple and effective way; heat treatment causes PVA to undergo hydroxy-dehydrating etherification (thermal cross-linking) and lose solubility, thus obtaining water-resistant PVA films.[16−18]

Nanofillers are ideal reinforcement materials that can achieve the combination of strength and toughness. To endow PVA films with antibacterial properties, adding a nano-antibacterial agent is a simple and effective way. Nano-ZnO is an inorganic antibacterial agent that is widely used in antibacterial packaging.[19] It is non-toxic and safe, having been identified by the U.S. Food and Drug Administration (FDA) as

https://doi.org/10.1021/acsomega.4c07173
ACS Omega 2024, 9, 50403−50413

a generally recognized as safe (GRAS) nanomaterial.[20,21] ZnO nanopillars (ZnO NPs) are a kind of ZnO nanomaterial that not only possesses the enhancements of nanomaterials but also has excellent antibacterial activity. ZnO NPs with a large length-to-diameter ratio can form bridge connections in the polymer matrix, thus achieving a better strengthening effect.[22] Furthermore, ZnO NPs can improve the strength of hydroxy-containing polymers (PVA, cellulose, and chitosan) by forming hydrogen bonds with them due to the available surface oxygen vacancies.[23−25] Therefore, adding ZnO NPs to the PVA film matrix can not only endow the film material a certain antibacterial property but also enhance the effect of the film material.

Among the preparation methods of nanocomposite materials, the blending method is commonly used at present, because of its simplicity and easy operation and the good properties of the prepared materials.[26−29] Therefore, PVA was used as the matrix, and ZnO NPs were used as the reinforcement material and the antibacterial agent; films of the PVA/ZnO NP composite were fabricated while employing the approach of blending, and the PVA/ZnO NPs-H films were fabricated by heat treatment. In addition, the ZnO addition amounts and heat treatment were systematically studied to better define their effects on the water resistance and mechanical properties of the composite films. The novelties of the present study lie in the following: (1) thanks to ZnO NPs, the prepared PVA-based composite films possess antibacterial properties, and their physicochemical properties are also enhanced, especially the mechanical properties; (2) the heat treatment not only confers on the films good water resistance but also further enhances the mechanical properties. Therefore, the current investigation revealed a straightforward method for producing PVA-based antibacterial packaging film materials with resistance to water, environmental friendliness, and high strength for applications in wet environments. These materials have a great deal of potential for use in green packaging.

2. EXPERIMENTAL SECTION

2.1. Materials and Reagents. All chemicals were of analytical grade and used as received. Zinc acetate dihydrate [$Zn(CH_3COO)_2{\cdot}2H_2O$] and PVA powder (with an average degree of polymerization of 2400−2500 and degree of alcoholysis of 98.0−99.8%) were procured from Sinopharm Chemical Reagent Co., Ltd. (Shanghai, China). Guanghua Sci-Tech Co., Ltd. (China) provided hexamethylenetetramine ($C_6H_{12}N_4$). Nanometer ZnO was supplied by Shanghai Aladdin Bio-Chem Technology Co., Ltd. (China). Shanghai Luwei Technology Co., Ltd. (China) provided *Escherichia coli* (ATCC 25922) and *Staphylococcus aureus* [CMCC(B)26003] for the study. Fresh apples and polyethylene (PE) plastic wrap were obtained from Walmart (Guangxi, China). All of the aqueous solutions were prepared using deionized water.

2.2. Fabrication of ZnO NPs. Briefly, 20 mmol/L $Zn(CH_3COO)_2$ solution and 20 mmol/L $C_6H_{12}N_4$ solution were prepared with deionized water, respectively. A 0.1 wt % nano-ZnO aqueous dispersion solution was prepared with deionized water. As per procedure, ZnO NPs were fabricated by mixing 100 mL of $Zn(CH_3COO)_2$ solution (20 mmol/L), 100 mL of $C_6H_{12}N_4$ solution (20 mmol/L), and 1 mL of nano-ZnO aqueous dispersion (0.1 wt %) in the hydrothermal reactor, and the temperature was kept at 90 °C for 3 h. ZnO NP powder was obtained by drying the particles after they were washed with deionized water.

2.3. Fabrication of PVA/ZnO NP Composite Films. The ZnO NP powder prepared in section 2.2 was ultrasonically dispersed into deionized water to obtain 1 wt % ZnO NP aqueous dispersion solution. A 4 wt % PVA aqueous solution was prepared with deionized water at 85 °C. Under ambient conditions, the dispersion of ZnO NPs was mixed with PVA aqueous solution via droplets while subject to continuous stirring, facilitating the formation of a homogenized mixed solution [m(ZnO NPs)/m(PVA) = 0 (pure PVA), 0.2, 0.5, 0.8, 1.0, and 1.5 wt %]. After the two solutions were fully mixed, the bubbles were eliminated using ultrasonication for 30 min. Subsequently, the mixture was introduced into a mold (depth of 3 mm) and horizontally positioned within a vacuum drying oven set at 60 °C, enabling the fabrication of PVA/ZnO NP composite films before undergoing any heat treatment processes. The final PVA/ZnO NP composite films were then obtained by heat treatment for 1 h at 165 °C in the oven. Figure S1 of the Supporting Information illustrates the steps involved in fabricating PVA/ZnO NP composite films both before and after heat treatment. The films of the PVA/ZnO NP composite were designated as PVA/ZnO NPs-1.5, PVA/ZnO NPs-1.0, PVA/ZnO NPs-0.8, PVA/ZnO NPs-0.5, PVA/ZnO NPs-0.2, and PVA/ZnO NPs-0 (pure PVA film) before heat treatment based on the ZnO NP content ranging from high to low. Similarly, following heat treatment, the films of the PVA/ZnO NP composite were designated as PVA/ZnO NPs-1.5-H, PVA/ZnO NPs-1.0-H, PVA/ZnO NPs-0.8-H, PVA/ZnO NPs-0.5-H, PVA/ZnO NPs-0.2-H, and PVA/ZnO NPs-0-H. For the next experiments, the produced film samples were kept at a constant temperature of 25 ± 1 °C and 50 ± 2% relative humidity (RH).

The characterization methods of materials are listed in the Supporting Information.

3. RESULTS AND DISCUSSION

3.1. X-ray Diffraction (XRD) Analyses and Morphological Characteristics of ZnO NPs. ZnO NPs were dispersed into deionized water to obtain an aqueous dispersion of 1 wt %, which was milky white (Figure 1a). The XRD results of ZnO NPs are displayed in Figure 1b. The characteristic diffraction peaks of ZnO NPs observed at 2θ values of 69.0°, 67.9°, 66.3°, 62.8°, 56.5°, 47.5°, 36.2°, 34.4°, and 31.7° were ascribed to the planes of typical hexagonal wurtzite of (201), (112), (200), (103), (110), (102), (101), (002), and (100), respectively.[30] The scanning electron microscopy (SEM) image of ZnO NPs' surface topography is depicted in Figure 1c. It is evident from the figure that ZnO NPs have a prolonged columnar shape with a diameter of around 100 nm and a length of 5−8 μm.

3.2. Results of Fourier Transform Infrared (FTIR), XRD, and Thermogravimetric Analyses of Composite Films. Figure 1d displays the composite films' FTIR spectra. The −OH stretching vibration absorption was identified as the cause of the broad peak bands near 3450 cm^{-1} of PVA/ZnO NPs-0, PVA/ZnO NPs-0-H, PVA/ZnO NPs-0.8, PVA/ZnO NPs-0.8-H, PVA/ZnO NPs-1.5, and PVA/ZnO NPs-1.5-H. This finding suggested that the samples contained a lot of −OH. The stretching vibration of ether bonds (C−O−C) resulting from dehydration etherification of −OH on PVA following thermal induction was identified as the cause of the distinctive absorption peak of PVA/ZnO NPs-0-H, PVA/ZnO NPs-0.8-H, and PVA/ZnO NPs-1.5-H at ∼1136 cm^{-1}.[18] Heat treatment modifies the structure of the films, as evidenced by

https://doi.org/10.1021/acsomega.4c07173
ACS Omega 2024, 9, 50403−50413

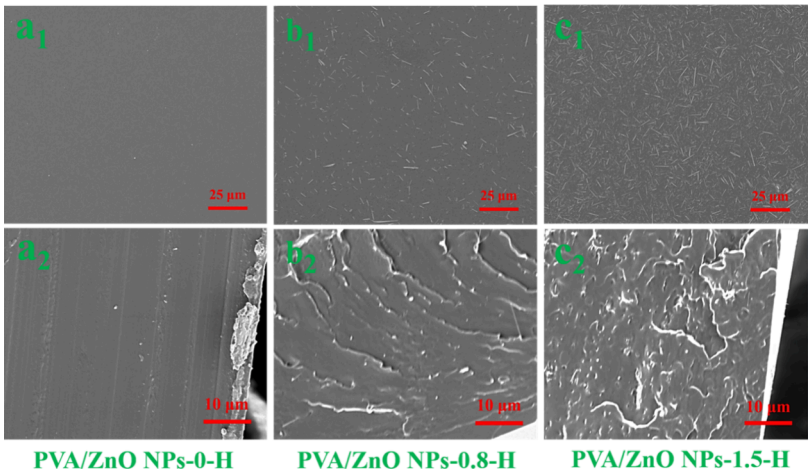

Figure 2. (a_1, b_1, and c_1) Surface and (a_2, b_2, and c_2) cross-sectional SEM images of PVA/ZnO NPs-0-H, PVA/ZnO NPs-0.8-H, and PVA/ZnO NPs-1.5-H films.

the absence of typical peaks of PVA/ZnO NPs-0, PVA/ZnO NPs-0.8, and PVA/ZnO NPs-1.5 at ∼1136 cm^{-1}. Heat treatment caused −OH on adjacent PVA molecular chains to dehydrate, etherify, and form a cross-linked network.[17]

The XRD results of the composite films of PVA/ZnO NPs are shown in Figure 1e. The films showed broad diffraction peaks at 2θ values of 19.6° both before and after heat treatment, which was attributed to PVA's semi-crystalline (110) plane.[31] In comparison to the films (PVA/ZnO NPs-0, PVA/ZnO NPs-0.8, and PVA/ZnO NPs-1.5) before heat treatment, the new diffraction peaks of the films (PVA/ZnO NPs-0-H, PVA/ZnO NPs-0.8-H, and PVA/ZnO NPs-1.5-H) after heat treatment appeared at 2θ = 11.4° and 22.6°, respectively; these peaks could be attributed to the formation of a new quasi-crystalline phase by dehydrating etherification (C−O−C) of PVA after heat treatment.[18] In addition, in comparison to pure PVA films (PVA/ZnO NPs-0 and PVA/ZnO NPs-0-H) before and after heat treatment, the new diffraction peaks of composite films (PVA/ZnO NPs-0.8, PVA/ZnO NPs-0.8-H, PVA/ZnO NPs-1.5, and PVA/ZnO NPs-1.5-H) appeared at 2θ = 31.7°, 56.5°, and 66.3°, respectively, which can exactly correspond to the (100), (110), and (200) diffraction peaks of typical hexagonal wurtzite, confirming that ZnO NPs were effectively distributed throughout the matrix of PVA to form composite films.

The thermogravimetric analysis (TGA) and derivative thermogravimetric (DTG) curves of PVA/ZnO NP composite films are displayed in panels f and g of Figure 1. Table S1 of the Supporting Information provides the associated maximum weight loss rate temperature (T_{max}) and the initial decomposition temperature (T_{onset}). All film samples had two stages of weightlessness between 150 and 450 °C, which showed the thermal characteristics of PVA. As illustrated in Figure 1f, weight loss due to volatilization of water was detected in all films in the first stage between 50 and 150 °C. The inclusion of ZnO NPs increased T_{onset} of the films, as indicated in Table S1 of the Supporting Information. This result was ascribed to ZnO NPs' strong thermal stability. Nonetheless, the inclusion of ZnO NPs appeared to lower T_{max} of the composite films, which may be attributed to their high thermal conductivity.[32] Figure 1g and Table S1 of the Supporting Information show that, while heat treatment had no discernible influence on film samples' T_{onset}, it clearly had an impact on T_{max}. After heat treatment, T_{max} of the film samples containing ZnO NPs was improved, which was due to the enhancement of the ZnO NPs. However, heat treatment slightly reduced T_{max} of the pure PVA film due to the dehydrating etherification of the hydroxyl group on PVA. Conclusively, ZnO NPs raised the thermal stability of the composite films.

3.3. Morphological Determination of Composite Films. SEM images of PVA/ZnO NPs-0-H, PVA/ZnO NPs-0.8-H, and PVA/ZnO NPs-1.5-H films' cross-section and surface topography are depicted in Figure 2. The PVA/ZnO NPs-0-H film's surfaces appeared to be comparatively smooth and flat, as seen by the SEM image (Figure 2a_1). ZnO NPs were added, and as a result, ZnO NPs were apparent on the PVA/ZnO NP composite film surface, and as the quantity of ZnO NPs increased, so did their density (panels b_1 and c_1 of Figure 2). From the inside, the flat and dense sectional structure of the PVA/ZnO NPs-0-H film can be clearly observed (Figure 2a_2). However, the dense section of the PVA/ZnO NPs-0.8-H film with ZnO NPs added became rough, and many microscale bright spots were observed in the section (Figure 2b_2), which were ZnO NP sections, dispersed in PVA. The cross-section of the PVA/ZnO NPs-1.5-H film (Figure 2c_2) shows clear flaws and aggregation of ZnO NPs following a surge in ZnO NP addition. This was due to phase separation brought on by an excessive amount of ZnO NP addition.[33] Consequently, it can be argued that adding the right amount of ZnO NPs will assist in enhancing the performance of PVA/ZnO NP films; however, adding too much ZnO NPs will cause some internal deterioration to the films.

3.4. Mechanical Properties of Composite Films. The thickness of the PVA/ZnO NP composite films is displayed in Figure S2 of the Supporting Information. The thickness of PVA/ZnO NP composite films ranged from 60 to 63 μm, and the presence of ZnO NPs resulted in a small rise in thickness. Additionally, the heat treatment induced a modest rise in the thickness of the composite films compared to their preheat treatment; this occurrence was brought on by the films' thermal shrinkage. The testing process for the mechanical properties of PVA/ZnO NP composite films can be referred to in Figure S3 of the Supporting Information. The PVA/ZnO NP composite films' elongation at break (EB) and tensile strength (TS) values are displayed in Figure 3a prior to heat

https://doi.org/10.1021/acsomega.4c07173
ACS Omega 2024, 9, 50403−50413

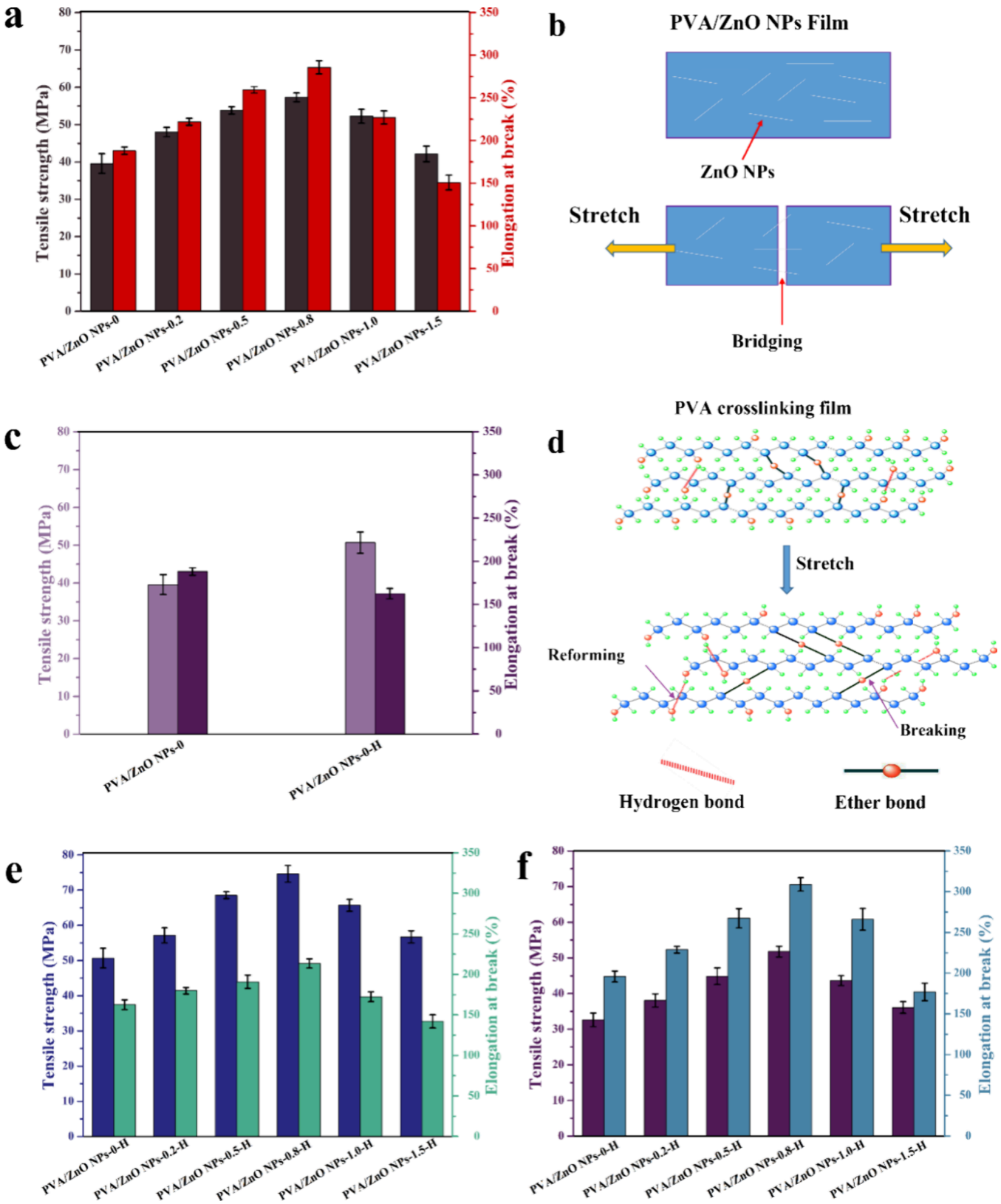

Figure 3. (a) Mechanical properties and (b) stretching resistance mechanism of the PVA/ZnO NP composite films (before heat treatment), (c) mechanical properties of the PVA films (both before and after heat treatment), (d) PVA film's stretching resistance mechanism (after heat treatment), and (e) dry and (f) humid mechanical properties of the PVA/ZnO NP composite films (after heat treatment).

treatment in the dry condition. The EB and TS values of PVA/ZnO NP composite films increased initially and then declined as the ZnO NP content increased, most likely as a result of agglomeration due to the excessive addition of ZnO NPs. Prior to heat treatment, the PVA/ZnO NPs-0.8 film had the best EB and TS values (285.77% and 57.33 MPa, respectively) among

https://doi.org/10.1021/acsomega.4c07173
ACS Omega 2024, 9, 50403−50413

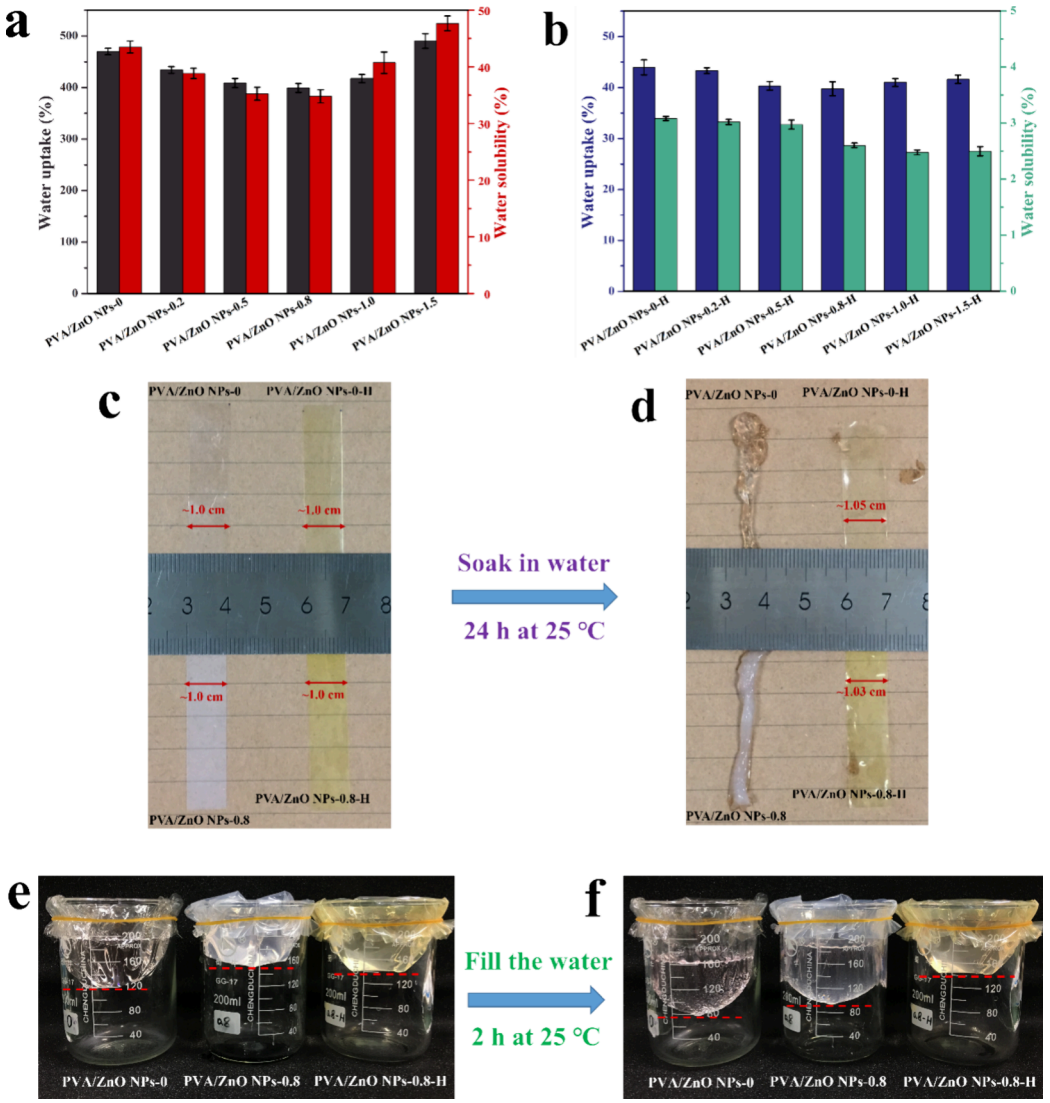

Figure 4. PVA/ZnO NP composite films' water uptake and solubility (a) before and (b) after heat treatment and photographs of the films of PVA/ZnO NPs-0, PVA/ZnO NPs-0-H, PVA/ZnO NPs-0.8, and PVA/ZnO NPs-0.8-H, with the photographs (c) depicting the samples before the water uptake test, (d) illustrating the samples after the water uptake test, (e) displaying the samples at the beginning of the water-filling test, and (f) portraying the samples at the end of the water-filling test for the PVA/ZnO NP composite films.

the PVA/ZnO NP composite films. Correspondingly, the PVA/ZnO NPs-0.8 film's EB and TS values were 44.81 and 51.82% higher than those of the PVA/ZnO NPs-0 film, which was caused by the ZnO NPs' enhancement. Figure 3b shows the stretching resistance mechanism of the PVA/ZnO NP composite films under stress. The mechanical properties of PVA/ZnO NP composite films were significantly enhanced over the stretching process due to the huge length-to-diameter ratio of ZnO NPs, which formed numerous bridge connection effects in the film matrix.[22,34] Subsequently, the relationship between heat treatment and mechanical properties of the PVA film was studied (Figure 3c). As demonstrated in the figure, the TS values of the PVA film were enhanced by heat treatment. Figure 3d exhibits the stretching resistance mechanism of the PVA film after heat treatment under stress. In detail, the PVA molecular chain is connected by ether bonds (C−O−C) that form following the dehydration and etherification of the hydroxyl group (−OH). This network structure helps to distribute the stress of the PVA film while stretching, increasing its mechanical properties.[18]

The heat-treated PVA/ZnO NP composite films' EB and TS values are depicted in Figure 3e in the state of dryness. It is evident that the PVA/ZnO NP composite films' TS values have improved significantly following heat treatment. The PVA/ZnO NPs-0.8-H film revealed the best TS values (74.63 MPa), which were 30.18 and 88.51% higher than those of PVA/ZnO NPs-0.8 and PVA/ZnO NPs-0 films correspondingly; this phenomenon was due to the synergistic enhancement of the bridge connection effect formed by ZnO NPs and the network structure formed by dehydration etherification of the hydroxyl group. The heat treatment of the PVA/ZnO NP composite films resulted in a predictable modest drop in their EB values. This decrease was primarily caused by the heat treatment's enhanced crystallinity, which, in turn, increased the composite films' brittleness.[35] Furthermore, the heat-treated PVA/ZnO NP composite films can still maintain excellent mechanical properties under the condition of complete immersion in water and wetting, such as the PVA/ZnO NPs-0.8-H film (TS, 52.85 MPa; EB, 308.88%) (Figure 3f). The PVA/ZnO NP composite films before heat treatment,

https://doi.org/10.1021/acsomega.4c07173
ACS Omega 2024, 9, 50403−50413

Table 1. Comparison of the Mechanical Properties of the PVA/ZnO NP Composite Films, in Both Dry and Humid Conditions, to the Published PVA-Based Packaging Films[a]

sample film	additives	dry tensile strength (MPa)/ enhancement ratio (%)	humid tensile strength (MPa)	reference
CMC/PVA	caroxymethyl cellulose	68.5/79.1	-	36
CNC/PVA/AgNP	cellulose nanocrystals and silver nanoparticles	73/55	-	37
lignin/PVA	lignin sphere	112/47	-	38
PVA/PEDOT:PSS/Ag NWs	silver nanowires	62.39/33.45	-	39
PVA/a-CMF	aldehyde rice straw cellulose microfiber	37.54/45.05	-	40
PVA/CNC	rod-shaped cellulose nanocrystals	44.84/42.51	-	41
PVA/BA	boric acid	82.1/69.3	-	42
PVA/ECNC	quaternized cellulose nanocrystals	45.4/37.2	-	43
PVA/ZnO NPs-0.8-H	ZnO nanopillars	74.63/88.51	52.85	this work

[a]Experimental conditions in the reported studies were not identical. "-" indicates that no relevant data are found in the reference.

however, absorbed water and inflated considerably after being soaked in water (Figure 4d), which rendered it difficult to investigate their mechanical properties. The results illustrated that the PVA/ZnO NP composite films after heat treatment possessed excellent water resistance because of the network structure formed by thermal cross-linking of PVA.[17] In particular, the stepwise enhancement effect of ZnO NPs and thermal cross-linking on the PVA film are clearly shown in Figure S4 of the Supporting Information.

The mechanical properties of the PVA-based composite films fabricated in this work are contrasted with those of their predecessors, and Table 1 lists the tensile strength values of film materials in both dry and humid situations. Outstanding tensile strength values were shown by the PVA/ZnO NPs-0.8-H film produced in this work in both dry and humid environments. Among the PVA-based films listed in this table, the PVA/ZnO NPs-0.8-H film differentiated out for its excellent humid tensile strength. These characteristics were attributed to the combining impact of ZnO NPs and mechanical attributes of the PVA film. The present approach is favored over others because of its facile method for the fabrication of PVA-based films with improved water resistance and excellent strength.

3.5. Wettability of the Composite Films. The water contact angle (WCA) of the PVA/ZnO NP composite films is depicted in Figure S5 of the Supporting Information. It can be observed from the figure that, with increasing content of ZnO NPs, the WCA of the PVA/ZnO NP composite films also improved. Excellent hydrophilicity was exhibited by the WCA (~57.55°) of the PVA/ZnO NPs-0 film without ZnO NPs. The introduction of ZnO NPs into PVA/ZnO NP composite films induces surface roughness, which enhances the hydrophobic nature of the film. This is evident in the increase of the WCA to approximately 69.66° in the PVA/ZnO NPs-0.8 film at a ZnO NP content of 0.8 wt %. This demonstrates that the inclusion of ZnO NPs reduces the hydrophilic properties of the PVA film.[44] Moreover, the reduction of hydrophilic hydroxyl groups on the PVA molecular chain by dehydration etherification resulted in a further enhancement of the WCA of the heat-treated PVA/ZnO NP composite films.[45]

Figure 4a displays the water uptake (WU) and water solubility (WS) of the PVA/ZnO NP composite films prior to heat treatment. The WU and WS of the PVA/ZnO NP composite films first reduced as the ZnO NP content grew, but later, they increased again. This suggests that adding the right amount of ZnO NPs can improve the composite film's compactness, which will help WU and WS decrease. Among them, the PVA/ZnO NPs-0.8 film showed the lowest WU and WS but still up to 399.27 and 34.85%, respectively. The results revealed that the PVA/ZnO NP composite films without heat treatment had a high hydrophilicity. On the other hand, following heat treatment, the WU and WS of the PVA/ZnO NP composite films were significantly decreased (Figure 4b). The PVA/ZnO NPs-0.8-H film exhibited the optimal WU (39.77%) and WS (2.54%), which corresponded to 92.71 and 90.04% lower than the PVA/ZnO NPs-0.8 film. The reason for this was that the PVA/ZnO NP composite films' water absorption and swelling degree were decreased and the cross-linked network structure created by the dehydration and etherification of PVA following heat treatment hindered the films from dissolving in water.[45] The films of PVA/ZnO NPs-0, PVA/ZnO NPs-0-H, PVA/ZnO NPs-0.8, and PVA/ZnO NPs-0.8-H are shown in panels c and d of Figure 4, both before and after the WU test. It was evident that the PVA/ZnO NPs-0 and PVA/ZnO NPs-0.8 films had swelled into a mass, while the PVA/ZnO NPs-0-H and PVA/ZnO NPs-0.8-H films had not inflated. Furthermore, the water-filling test findings revealed that, after 2 h, there was significant swelling in the PVA/ZnO NPs-0.8 and PVA/ZnO NPs-0 films and water droplets infiltrated the films (panels e and f of Figure 4). It is also evident from panels e and f of Figure 4 that, after 2 h of the water filling test, practically little change was seen in the PVA/ZnO NPs-0.8-H film. The findings further revealed that the heat-treated PVA/ZnO NP composite films exhibited excellent resistance to water swelling and could be employed for packaging applications in humid environments.

3.6. Transparency and Barrier Properties of Composite Films. The ultraviolet/visible (UV/vis) transmittance spectrum of the PVA/ZnO NP composite films at 200−800 nm wavelength is depicted in Figure S6a of the Supporting Information. The film of PVA/ZnO NPs-0 demonstrated excellent optical transparency at 250−800 nm wavelength, with an average transparency greater than 90%. ZnO NPs have a detrimental influence on PVA film transparency, as evidenced by the transmittance of the PVA/ZnO NP composite films, which rapidly decreased as the content of ZnO NPs increased. The transmittance of the composite films following heat treatment was basically the same at wavelengths larger than 550 nm compared to the films before heat treatment. However, the transmittance of the heat-treated composite films decreased seriously at wavelengths less than 550 nm, which was brought about by heat treatment's tendency to cause

https://doi.org/10.1021/acsomega.4c07173
ACS Omega 2024, 9, 50403−50413

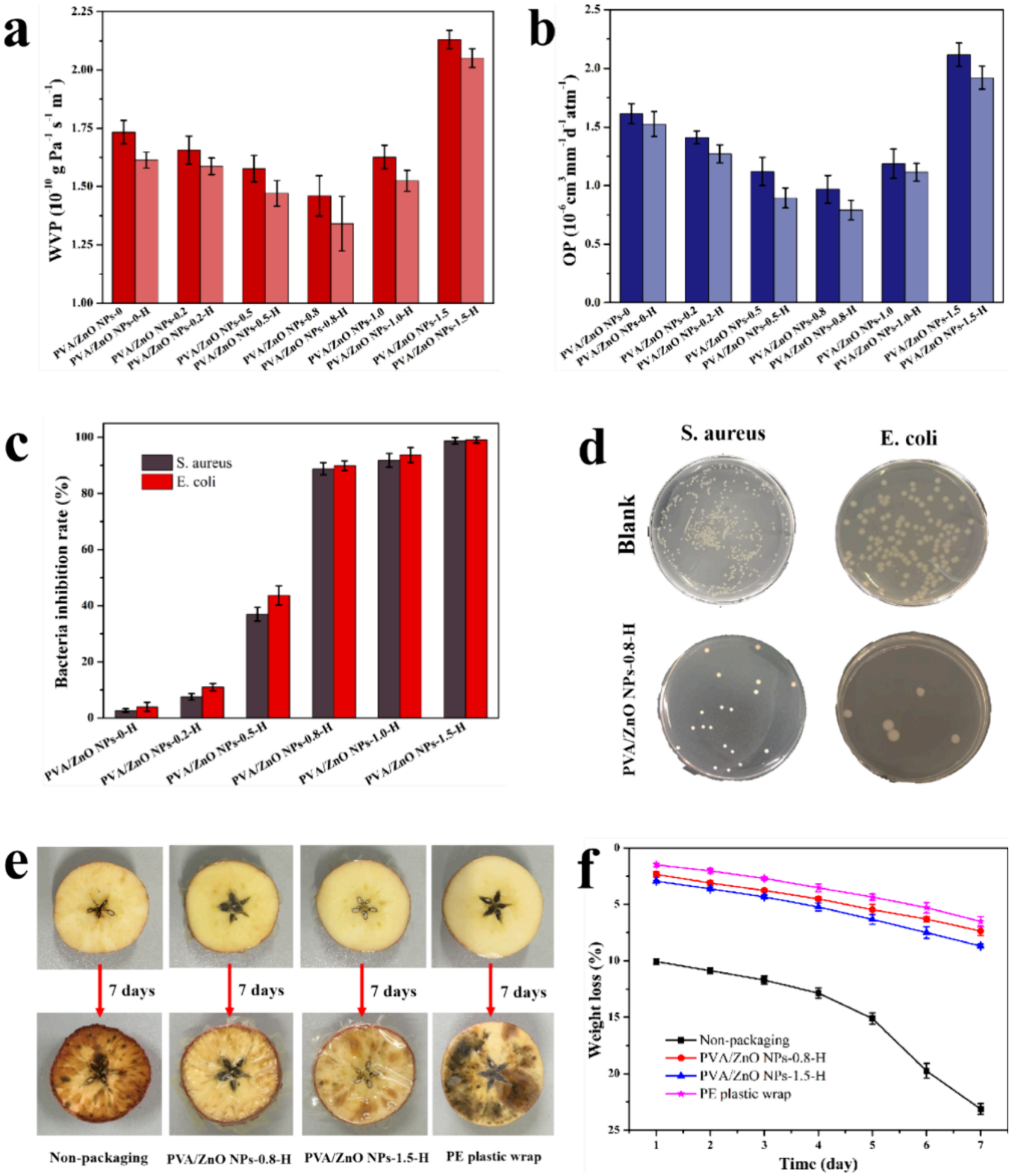

Figure 5. (a) Water vapor permeability and (b) oxygen permeability of the PVA/ZnO NP composite films, (c) PVA/ZnO NP composite films' rates of bacterial inhibition against *S. aureus* and *E. coli* following heat treatment, (d) photographs of the PVA/ZnO NPs-0.8-H film's antibacterial test against *S. aureus* and *E. coli*, with the control group shown by the black samples, (e) effects of several packing techniques on half-cut apples' preservation after 7 days in preservation: non-packaging, PE plastic wrap, PVA/ZnO NPs-0.8-H, and PVA/ZnO NPs-1.5-H films, and (f) weight loss rate of half-cut apples during 7 days of preservation.

composite films' color to turn yellow (Figure S6b of the Supporting Information). These results revealed that the light transmittance of the composite films was negatively impacted by the ZnO NPs and heat treatment. In general, the films of the PVA/ZnO NP composite in the present study possessed good light transmittance.

https://doi.org/10.1021/acsomega.4c07173
ACS Omega 2024, 9, 50403−50413

The water vapor permeability (WVP) and oxygen permeability (OP) of the PVA/ZnO NP composite films are depicted in panels a and b of Figure 5. Before heat treatment, the WVP of the PVA/ZnO NP composite films first declined and then increased as the ZnO NP content increased (Figure 5a). The WVP of the PVA/ZnO NPs-0.8 film was the lowest among them at 1.46×10^{-10} g Pa^{-1} s^{-1} m^{-1}, while the WVP of the PVA/ZnO NPs-1.5 film was the highest at 2.13×10^{-10} g Pa^{-1} s^{-1} m^{-1}. This result showed that, while adding a large amount of ZnO NPs can lead to flaws in the composite films, which lowers the barrier of the composite films to water vapor, adding too few ZnO NPs can increase the density of the composite films while enhancing its barrier to water vapor.[46] After heat treatment, the barrier of the PVA/ZnO NP composite films to water vapor was further enhanced (Figure 5a). The optimal WVP was observed at 1.33×10^{-10} g Pa^{-1} s^{-1} m^{-1} in the PVA/ZnO NPs-0.8-H film, and it was 8.91% lower than that in the PVA/ZnO NPs-0.8 film. This was primarily because heat treatment dehydration etherified the hydroxyl group on PVA, decreasing the hydrophilicity of the PVA/ZnO NP composite films. Furthermore, the PVA/ZnO NP composite films' OP fluctuation pattern paralleled WVP's (Figure 5b). The PVA/ZnO NPs-0.8-H film demonstrated the best OP at 0.79×10^{-5} cm^3 mm^{-1} day^{-1} atm^{-1} among all, and it was 50.93% less than the film of PVA/ZnO NPs-0. This resulted from the appropriate loading of ZnO NPs and heat treatment to improve the composite films' compactness.

3.7. Antibacterial Activity of Composite Films. The antibacterial activity of the PVA/ZnO NP composite films against *S. aureus* and *E. coli* following heat treatment is depicted in panels c and d of Figure 5. The PVA/ZnO NPs-0-H film without ZnO NPs inhibited *E. coli* and *S. aureus* bacteria at rates of 3.95 and 2.66%, respectively (Figure 5c). This inhibition may have been caused by an electrostatic interaction between the film's surface and the surface of the microbial cell membrane.[47] The PVA/ZnO NP composite films' bacteriostatic activity against *S. aureus* and *E. coli* considerably increased with an increase in the content of ZnO NPs. When the content of ZnO NPs was 0.8 wt %, the PVA/ZnO NPs-0.8-H film inhibited *E. coli* and *S. aureus* up to 91.59 and 90.93%, respectively (Figure 5c). The digital photos of the PVA/ZnO NPs-0.8-H film's antibacterial test against *E. coli* and *S. aureus* are displayed in Figure 5d to further illustrate the bacteriostatic activity. The findings of the study revealed that ZnO NPs gave the antibacterial activity of the PVA-based composite film. The antibacterial mechanism of ZnO nanoparticles is currently the subject of numerous theories. However, the prevalent ideas link the release of Zn^{2+} and the production of reactive oxygen species [ROS, such as superoxide anion (O_2^-), hydroxyl radicals ($OH^•$), and H_2O_2] to bacterial inactivation.[48,49] In this study, ZnO NPs are mainly used as a strengthening material to improve the mechanical properties of the composite films, and the addition amount is very small. Correspondingly, the amount of ZnO NPs on the surface of the composite films is less. In addition, in the previous study, we prepared a cellulose-based antimicrobial film incroporated with ZnO NPs on the surface, and the maximum mobility of zinc ions in water of the ZnO NPs was 4.3 mg L^{-1}, which was lower than the minimum inhibitory concentration of zinc ions.[23] Therefore, even if ZnO migrates, it is very small and does not pose a potential risk to human health.

3.8. Packaging Application of Composite Films. The preservation effect of the PVA/ZnO NP composite films after heat treatment in food packaging was investigated using half-cut apples as models for packaging testing. The results are displayed in panels e and f of Figure 5. The half-cut apples without film packing showed an atrophic and wrinkled surface with the beginning of fruit rotting after being stored for 7 days at 25 °C and 60% RH (Figure 5e). Similarly, the cut surface of the apple packaged with PE plastic wrap also experienced serious rot and mildew (Figure 5e), which was mainly caused by the lack of antibacterial function of PE plastic wrap. However, the apples packaged with PVA/ZnO NTP-0.8-H and PVA/ZnO NTP-1.5-H films remained full in appearance with only slight browning appearing on the cut surface (Figure 5e), which was mainly due to the good barrier and antibacterial properties of PVA/ZnO NP composite films.[50] The weight loss rate curve for half-cut apples throughout the 7 day packing test is depicted in Figure 5f. It can be observed from the figure that the weight loss rate of the half-cut apples without film wrapping expanded daily, reaching as high as 9.85% on the first day due to water evaporation. As a result, the sixth day had the highest stage weight loss rate, which might be caused by the decay of the apple. The half-cut apples packaged with the films (PVA/ZnO NPs-0.8-H, PVA/ZnO NPs-1.5-H, and PE plastic wrap) displayed a constant daily weight loss rate (Figure 5f), which was due to the existence of films preventing the evaporation of water in the apples. After 7 days, the weight loss rates of the half-cut apples packaged without film and with PVA/ZnO NPs-0.8-H film, PVA/ZnO NPs-1.5-H film, or PE plastic wrap were 23.13, 7.35, 8.69, and 7.03%, respectively. Despite having the lowest rate of weight loss, the half-cut apples covered in PE plastic wrap had significant deterioration after 7 days. This was because the PE plastic wrap lacked antibacterial activity. The research findings indicated that the heat-treated PVA/ZnO NP composite films demonstrated a certain level of application value in the antibacterial packaging film industry and successfully packed and preserved fruits.

4. CONCLUSION

In summary, PVA/ZnO NP composite films were successfully fabricated while employing the approaches of blending and heat treatment. The PVA/ZnO NP composite films were evaluated for a variety of attributes, such as wettability, mechanical properties, in humid and dry environments, barrier properties, antibacterial activity, and the package preservation effect. The films of the PVA/ZnO NP composite revealed excellent water resistance following heat treatment. Furthermore, the films showed excellent tensile strength under both dry (74.63 MPa) and humid (52.85 MPa) environments at 0.8 wt % ZnO NPs content following heat treatment. The synergistic effect of the ZnO NPs' bridge connection enhancement and the heat-induced cross-linked network structure between PVA molecular chains were primarily responsible for the increased wet strength of the films. The PVA/ZnO NP composite films with ZnO NP content above 0.8 wt % demonstrated outstanding bactericidal activities against *E. coli* and *S. aureus*. In addition, it was observed that PVA/ZnO NP composite films significantly inhibited microbial growth in the process of packaging and preservation of half-cut apples. The current study revealed significant potential applications in green packaging and offered a straightforward method for producing PVA-based antibacterial packaging films

https://doi.org/10.1021/acsomega.4c07173
ACS Omega 2024, 9, 50403−50413

with excellent water resistance and strength for applications in wet and humid environments.

■ ASSOCIATED CONTENT

Supporting Information

The Supporting Information is available free of charge at https://pubs.acs.org/doi/10.1021/acsomega.4c07173.

Characterization methods of materials and preparation diagram, thickness, photographs of the stretch test, stress−strain curves, water contact angles, light transmittance, and thermal performance data of PVA/ZnO NP composite films.

■ AUTHOR INFORMATION

Corresponding Authors

Pingxiong Cai − *Guangxi Key Laboratory of Green Chemical Materials and Safety Technology, Guangxi Engineering Research Center for New Chemical Materials and Safety Technology, College of Petroleum and Chemical Engineering, Beibu Gulf University, Qinzhou 535011, China*; Email: pingxiongcai@bbg.edu.cn

Yuanfeng Pan − *Guangxi Colleges and Universities Key Laboratory of New Technology and Application in Resource Chemical Engineering, School of Chemistry and Chemical Engineering, Guangxi University, Nanning 530004, China*; orcid.org/0000-0002-5002-5383; Email: panyf@gxu.edu.cn

Authors

Yuanjian Xie − *Guangxi Key Laboratory of Green Chemical Materials and Safety Technology, Guangxi Engineering Research Center for New Chemical Materials and Safety Technology, College of Petroleum and Chemical Engineering, Beibu Gulf University, Qinzhou 535011, China*; orcid.org/0009-0000-8112-4336

Xiaofeng Cao − *Guangxi Key Laboratory of Green Chemical Materials and Safety Technology, Guangxi Engineering Research Center for New Chemical Materials and Safety Technology, College of Petroleum and Chemical Engineering, Beibu Gulf University, Qinzhou 535011, China*

Bo Chen − *Guangxi Key Laboratory of Green Chemical Materials and Safety Technology, Guangxi Engineering Research Center for New Chemical Materials and Safety Technology, College of Petroleum and Chemical Engineering, Beibu Gulf University, Qinzhou 535011, China*; orcid.org/0000-0002-2266-2529

Complete contact information is available at: https://pubs.acs.org/10.1021/acsomega.4c07173

Notes

The authors declare no competing financial interest.

■ ACKNOWLEDGMENTS

This work was supported by the Middle-Aged and Young Teachers' Basic Ability Promotion Project of Guangxi (2023KY0442) and the National Natural Science Foundation of China (22068006). This work was also funded by the Guangxi Key Laboratory of Green Chemical Materials and Safety Technology, College of Petroleum and Chemical Engineering, Beibu Gulf University (2022ZZKT05 and 22KYQD15). The authors also acknowledged the Innovation-Driven Development Special Fund Project of Guangxi (AA23062016-4) and the Counterpart Support Discipline Construction Project by Guangxi University (2023B04).

■ REFERENCES

(1) Wei, R.; Zimmermann, W. Microbial enzymes for the recycling of recalcitrant petroleum-based plastics: How far are we? *Microb. Biotechnol.* **2017**, *10* (6), 1308−1322.

(2) Zia, J.; Paul, U. C.; Heredia-Guerrero, J. A.; Athanassiou, A.; Fragouli, D. Low-density polyethylene/curcumin melt extruded composites with enhanced water vapor barrier and antioxidant properties for active food packaging. *Polymer* **2019**, *175*, 137−145.

(3) Horodytska, O.; Valdes, F. J.; Fullana, A. Plastic flexible films waste management—A state of art review. *Waste Manage.* **2018**, *77*, 413−425.

(4) Li, Y.; Wang, S.; Qian, S.; Liu, Z.; Weng, Y.; Zhang, Y. Depolymerization and Re/Upcycling of Biodegradable PLA Plastics. *ACS Omega* **2024**, *9* (12), 13509−13521.

(5) Karanth, S.; Feng, S. Y.; Patra, D.; Pradhan, A. K. Linking microbial contamination to food spoilage and food waste: The role of smart packaging, spoilage risk assessments, and date labeling. *Front. Microbiol.* **2023**, *14*, 1198124.

(6) Yan, T.; Wang, X.; Qiao, Y. Strategy to Antibacterial, High-Mechanical, and Degradable Polylactic Acid/Chitosan Composite Film through Reactive Compatibilization via Epoxy Chain Extender. *ACS Omega* **2024**, *9* (25), 27312−27320.

(7) Shaikh, S.; Yaqoob, M.; Aggarwal, P. An overview of biodegradable packaging in food industry. *Curr. Res. Food Sci.* **2021**, *4*, 503−520.

(8) Liu, S. J.; Gao, X. Q.; Fan, H.; Zhang, M. T.; Waterhouse, G. I. N.; Zhu, S. H. Green and recyclable graphitic carbon nitride/chitosan/polyvinyl alcohol photocatalytic films with efficient antibacterial activity for fruit packaging. *Int. J. Biol. Macromol.* **2023**, *236*, 123974.

(9) Abdullah, Z. W.; Dong, Y.; Davies, I. J.; Barbhuiya, S. PVA, PVA Blends, and Their Nanocomposites for Biodegradable Packaging Application. *Polym.-Plast. Technol.* **2017**, *56* (12), 1307−1344.

(10) Oun, A. A.; Shin, G. H.; Rhim, J. W.; Kim, J. T. Recent advances in polyvinyl alcohol-based composite films and their applications in food packaging. *Food Packag. Shelf Life* **2022**, *34*, 100991.

(11) Kang, S. L.; Wang, H. L.; Xia, L.; Chen, M. M.; Li, L. L.; Cheng, J. F.; Li, X. J.; Jiang, S. T. Colorimetric film based on polyvinyl alcohol/okra mucilage polysaccharide incorporated with rose anthocyanins for shrimp freshness monitoring. *Carbohydr. Polym.* **2020**, *229*, 115402.

(12) Gigli, M.; Lotti, N.; Gazzano, M.; Siracusa, V.; Finelli, L.; Munari, A.; Dalla Rosa, M. Fully Aliphatic Copolyesters Based on Poly(butylene 1,4-cyclohexanedicarboxylate) with Promising Mechanical and Barrier Properties for Food Packaging Applications. *Ind. Eng. Chem. Res.* **2013**, *52* (36), 12876−12886.

(13) Hussain, R.; Batool, S. A.; Aizaz, A.; Abbas, M.; Ur Rehman, M. A. Biodegradable Packaging Based on Poly(vinyl Alcohol) and Carboxymethyl Cellulose Films Incorporated with Ascorbic Acid for Food Packaging Applications. *ACS Omega* **2023**, *8* (45), 42301−42310.

(14) Li, L.; Xu, X.; Liu, L.; Song, P.; Cao, Q.; Xu, Z.; Fang, Z.; Wang, H. Water governs the mechanical properties of poly(vinyl alcohol). *Polymer* **2021**, *213*, 123330.

(15) Wang, C.; Shu, H.; Sun, D.; Yang, L.; Song, C.; Zhang, X.; Chen, D.; Ma, Y.; Yang, W. Synthesis of poly(maleic anhydride-co-vinyl chloride) crosslinked microspheres and its superior enhancement in mechanical strength and antibacterial activity for poly(vinyl alcohol) composite films. *Polymer* **2024**, *298*, 126918.

(16) Sonker, A. K.; Verma, V. Influence of crosslinking methods toward poly(vinyl alcohol) properties: Microwave irradiation and conventional heating. *J. Appl. Polym. Sci.* **2018**, *135* (14), 46125.

(17) Xie, Y. J.; Pan, Y. F.; Cai, P. X. Hydroxyl crosslinking reinforced bagasse cellulose/polyvinyl alcohol composite films as biodegradable packaging. *Ind. Crops Prod.* **2022**, *176*, 114381.

(18) Xie, Y. J.; Pan, Y. F.; Cai, P. X. Novel PVA-Based Porous Separators Prepared via Freeze-Drying for Enhancing Performance of Lithium-Ion Batteries. *Ind. Eng. Chem. Res.* **2020**, *59* (34), 15242−15254.
(19) Duan, L.; Yan, F.; Zhang, L.; Liu, B.; Zhang, Y.; Tian, X.; Liu, Z.; Wang, X.; Wang, S.; Tian, J.; Bao, H.; Liu, T. ZnO@Polyvinyl Alcohol/Poly(lactic acid) Nanocomposite Films for the Extended Shelf Life of Pork by Efficient Antibacterial Adhesion. *ACS Omega* **2022**, *7* (49), 44657−44669.
(20) Kumar, R.; Umar, A.; Kumar, G.; Nalwa, H. S. Antimicrobial properties of ZnO nanomaterials: A review. *Ceram. Int.* **2017**, *43* (5), 3940−3961.
(21) Smaoui, S.; Cherif, I.; Ben Hlima, H.; Khan, M. U.; Rebezov, M.; Thiruvengadam, M.; Sarkar, T.; Shariati, M. A.; Lorenzo, J. M. Zinc oxide nanoparticles in meat packaging: A systematic review of recent literature. *Food Packag. Shelf Life* **2023**, *36*, 101045.
(22) Xu, J. T.; Chen, X. Q.; Shen, W. H.; Li, Z. Spherical vs rod-like cellulose nanocrystals from enzymolysis: A comparative study as reinforcing agents on polyvinyl alcohol. *Carbohydr. Polym.* **2021**, *256*, 117493.
(23) Xie, Y. J.; Pan, Y. F.; Cai, P. X. Cellulose-based antimicrobial films incroporated with ZnO nanopillars on surface as biodegradable and antimicrobial packaging. *Food Chem.* **2022**, *368*, 130784.
(24) Zhao, S. W.; Zheng, M.; Sun, H. L.; Li, S. J.; Pan, Q. J.; Guo, Y. R. Construction of heterostructured g-C_3N_4/ZnO/cellulose and its antibacterial activity: Experimental and theoretical investigations. *Dalton Trans.* **2020**, *49* (12), 3723−3734.
(25) Yadav, S.; Mehrotra, G. K.; Dutta, P. K. Chitosan based ZnO nanoparticles loaded gallic-acid films for active food packaging. *Food Chem.* **2021**, *334*, 127605.
(26) Han, Z.-M.; Li, D.-H.; Yang, H.-B.; Zhao, Y.-X.; Yin, C.-H.; Yang, K.-P.; Liu, H.-C.; Sun, W.-B.; Ling, Z.-C.; Guan, Q.-F.; Yu, S.-H. Nacre-Inspired Nanocomposite Films with Enhanced Mechanical and Barrier Properties by Self-Assembly of Poly(Lactic Acid) Coated Mica Nanosheets. *Adv. Funct. Mater.* **2022**, *32* (32), 2202221.
(27) Zhou, L. P.; Tian, Y.; Xu, P.; Wei, H. J.; Li, Y. H.; Peng, H. X.; Qin, F. X. Effect of the selective localization of carbon nanotubes and phase domain in immiscible blends on tunable microwave dielectric properties. *Compos. Sci. Technol.* **2021**, *213*, 108919.
(28) Sharma, S.; Byrne, M.; Perera, K. Y.; Duffy, B.; Jaiswal, A. K.; Jaiswal, S. Active film packaging based on bio-nanocomposite TiO_2 and cinnamon essential oil for enhanced preservation of cheese quality. *Food Chem.* **2023**, *405*, 134798.
(29) Li, C.; Wang, B.; Shang, Z.; Yu, L.; Wei, C.; Wei, Z.; Sang, L.; Li, Y. High-Barrier Poly(butylene succinate-co-terephthalate) Blend with Poly(lactic acid) as Biodegradable Food Packaging Films. *Ind. Eng. Chem. Res.* **2023**, *62* (18), 7250−7261.
(30) Yang, X.; Wang, S. J.; Huang, Z. W.; Zhao, X. L.; Hu, J.; Li, Q.; He, J. L. Surface treated ZnO whisker optimizing the comprehensive performance of the self-adaptive dielectrics. *Compos. Sci. Technol.* **2023**, *233*, 109918.
(31) Selvi, J.; Mahalakshmi, S.; Parthasarathy, V.; Hu, C. C.; Lin, Y. F.; Tung, K. L.; Anbarasan, R.; Annie, A. A. Optical, thermal, mechanical properties, and non-isothermal degradation kinetic studies on PVA/CuO nanocomposites. *Polym. Compos.* **2019**, *40* (9), 3737−3748.
(32) Pan, Y. F.; Xie, Y. J.; Cai, P. X. Cellulose-based films reinforced by in-situ generated ZnO for antimicrobial packaging. *Cellulose* **2022**, *29* (17), 9375−9391.
(33) Zhang, X. Q.; Luo, W. H.; Xiao, N. Y.; Chen, M. J.; Liu, C. F. Construction of functional composite films originating from hemicellulose reinforced with poly(vinyl alcohol) and nano-ZnO. *Cellulose* **2020**, *27* (3), 1341−1355.
(34) Yu, H. Y.; Zhang, H.; Song, M. L.; Zhou, Y.; Yao, J. M.; Ni, Q. Q. From Cellulose Nanospheres, Nanorods to Nanofibers: Various Aspect Ratio Induced Nucleation/Reinforcing Effects on Polylactic Acid for Robust-Barrier Food Packaging. *ACS Appl. Mater. Interfaces* **2017**, *9* (50), 43920−43938.
(35) Lee, E. S.; Lei, D.; Devarayan, K.; Kim, B. S. High strength poly(vinyl alcohol)/poly(acrylic acid) cross-linked nanofibrous hybrid composites incorporating nanohybrid POSS. *Compos. Sci. Technol.* **2015**, *110*, 111−117.
(36) Youssef, H. F.; El-Naggar, M. E.; Fouda, F. K.; Youssef, A. M. Antimicrobial packaging film based on biodegradable CMC/PVA-zeolite doped with noble metal cations. *Food Packag. Shelf Life* **2019**, *22*, 100378.
(37) Fan, L.; Zhang, H.; Gao, M. X.; Zhang, M.; Liu, P. T.; Liu, X. L. Cellulose nanocrystals/silver nanoparticles: In-situ preparation and application in PVA films. *Holzforschung* **2020**, *74* (5), 523−528.
(38) Huang, J. B.; Guo, Q.; Zhu, R. N.; Liu, Y. Y.; Xu, F.; Zhang, X. M. Facile fabrication of transparent lignin sphere/PVA nanocomposite films with excellent UV-shielding and high strength performance. *Int. J. Biol. Macromol.* **2021**, *189*, 635−640.
(39) Yu, J. W.; Gu, W. H.; Zhao, H. Q.; Ji, G. B. Lightweight, flexible and freestanding PVA/PEDOT:PSS/Ag NWs film for high-performance electromagnetic interference shielding. *Sci. China Mater.* **2021**, *64* (7), 1723−1732.
(40) Feng, Z. X.; Xu, D.; Shao, Z. B.; Zhu, P.; Qiu, J. H.; Zhu, L. X. Rice straw cellulose microfiber reinforcing PVA composite film of ultraviolet blocking through pre-cross-linking. *Carbohydr. Polym.* **2022**, *296*, 119886.
(41) Li, L. L.; Wang, W. X.; Sun, J. F.; Chen, Z. Z.; Ma, Q. Y.; Ke, H. Z.; Yang, J. X. Improved properties of polyvinyl alcohol films blended with aligned nanocellulose particles induced by a magnetic field. *Food Packag. Shelf Life* **2022**, *34*, 100985.
(42) Zhang, S. T.; Wei, D. F.; Xu, X.; Guan, Y. Transparent, High-Strength, and Antimicrobial Polyvinyl Alcohol/Boric Acid/Poly Hexamethylene Guanidine Hydrochloride Films. *Coatings* **2023**, *13* (6), 1115.
(43) Meng, L. A.; Li, J. W.; Fan, X. Y.; Wang, Y. G.; Xiao, Z. F.; Wang, H. G.; Liang, D. X.; Xie, Y. J. Improved mechanical and antibacterial properties of polyvinyl alcohol composite films using quaternized cellulose nanocrystals as nanofillers. *Compos. Sci. Technol.* **2023**, *232*, 109885.
(44) Moghadam, S. G.; Parsimehr, H.; Ehsani, A. Multifunctional superhydrophobic surfaces. *Adv. Colloid Interface Sci.* **2021**, *290*, 102397.
(45) Bolto, B.; Tran, T.; Hoang, M.; Xie, Z. Crosslinked poly(vinyl alcohol) membranes. *Prog. Polym. Sci.* **2009**, *34* (9), 969−981.
(46) Yu, J. F.; Ruengkajorn, K.; Crivoi, D.-G.; Chen, C. P.; Buffet, J.-C.; O'Hare, D. High gas barrier coating using non-toxic nanosheet dispersions for flexible food packaging film. *Nat. Commun.* **2019**, *10*, 2398.
(47) Roy, S.; Rhim, J. W. Carboxymethyl cellulose-based antioxidant and antimicrobial active packaging film incorporated with curcumin and zinc oxide. *Int. J. Biol. Macromol.* **2020**, *148*, 666−676.
(48) Kim, I.; Viswanathan, K.; Kasi, G.; Thanakkasaranee, S.; Sadeghi, K.; Seo, J. ZnO Nanostructures in Active Antibacterial Food Packaging: Preparation Methods, Antimicrobial Mechanisms, Safety Issues, Future Prospects, and Challenges. *Food Rev. Int.* **2022**, *38* (4), 537−565.
(49) Sirelkhatim, A.; Mahmud, S.; Seeni, A.; Kaus, N. H. M.; Ann, L. C.; Bakhori, S. K. M.; Hasan, H.; Mohamad, D. Review on Zinc Oxide Nanoparticles: Antibacterial Activity and Toxicity Mechanism. *Nano-Micro Lett.* **2015**, *7* (3), 219−242.
(50) Kim, W.; Han, T.; Gwon, Y.; Park, S.; Kim, H.; Kim, J. Biodegradable and Flexible Nanoporous Films for Design and Fabrication of Active Food Packaging Systems. *Nano Lett.* **2022**, *22* (8), 3480−3487.

https://doi.org/10.1021/acsomega.4c07173
ACS Omega 2024, 9, 50403−50413